

DYNAMICS OF ROTOR SYSTEMS WITH FLUID ANNULAR SEALS

Davydov A.V., Degtiarev S.A., Ivanov A.V., Leontiev M.K.

The mathematical model of the hydrodynamic annular seal- the floating ring and methodology for investigation of the fluid pumps rotor dynamics is presented. The algorithm to determine hydrodynamic force and reaction of a seal as a part of the rotor system is given. By example of the high speed model rotor with the annular seal, the motion of the rotor shaft and the ring is investigated, the rotor stability boundary is obtained.

Key words: rotordynamics, annular seals, floating ring

Perspective direction to improve turbomachines is increase in their power due to increase in the rotor speed. As a result, decrease in overall and mass characteristics takes place, which is especially important for aviation engines. For example, it is well-known that a vane pump power increases in proportion to outer diameter of an impeller and rotating speed. At the present time perspectives to create the turbopumps of rocket engines with delivery pressure higher than 100 MPa, gas temperature at turbine inlet section up to 1500 K, operating speeds of the rotor surfaces of the seals more than 600 m/s are considered.

Prospects to increase the turbopumps rotor speed in order to raise efficiency of the pump units are highly estimated by both Russian and foreign specialists. Tendency towards rise in circumferential speed in the pumps and the turbines of the turbopumps may be seen in Figure 1 [1].

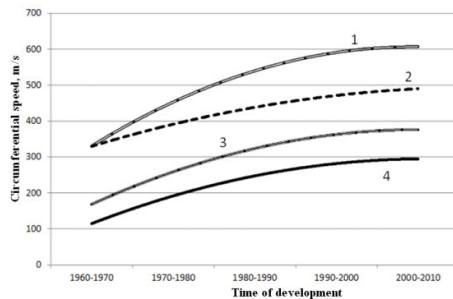


Figure 1. Tendency towards rise in circumferential speed in pumps and turbines of turbopumps

1 – circumferential speed on outer diameter of impellers of hydrogen pumps; 2 – circumferential speed on mean diameter of turbines of hydrogen turbopumps, 3 – circumferential speed on mean diameter of turbines of oxygen turbopumps, 4 – circumferential speed on outer diameter of impellers of oxygen turbopumps

Meanwhile, the rotors speeds reach 140000 rpm. Especially fast increase in circumferential speeds is typical of hydrogen pumps of oxygen-hydrogen liquid-propellant rocket engines.

Davydov Arkadiy V. - MAI, post-graduate student, e-mail: davidovarc@alfatran.com

Degtiarev Sergey A., - the scientific and technical centre of rotordynamics Alfa-Tranzit Ltd., course leader, e-mail: degs@alfatran.com

Ivanov Andrey V., KBKhA, deputy chief designer, candidate of technical science, e-mail: iav308@inbox.ru

Leontiev Michail K., -MAI, professor, Doctor of technical science, e-mail: lem@alfatran.com.

To lower volume losses, different seals are used in turbopumps. Hydrodynamic seals – different annular seals - are used more often. The implemented experimental research in balancing of the centrifugal pump rotor shows that the reason for an increased rotor vibration level is not so much its residual unbalance as influence of the supports and the annular seals [2]. Holding of additional balancing of the turbopump rotor at nominal regime with the badly designed and calculated seals' units doesn't improve its vibration characteristics, as a rule.

The seals of the channels of the hydrogen pumps influence the rotors dynamic characteristics significantly. For example, during development of the hydrogen turbopump of the SSME engine of the orbital transfer spaceship of repeated usage «Space Shuttle», defects of the rotor system related to the seals were revealed. It should be noticed that almost all the rotors used nowadays in the hydrogen pumps of the liquid-propellant engines work with an operating rotating speed exceeding the first critical speed, and the rotor of the hydrogen pump of the Japanese engine LE-7 sequentially passes three critical speeds when reaching the operating speed. Thus, the seals of the hydrogen channels at the certain moments of time work under conditions of increased vibration level of the rotor seal faces. Also, seals because of their quantity act as additional supports and hydrodynamic dampers. For example, damping of oscillations when passing critical speeds in the hydrogen pump of the VINCI engine, developed by Snecma company in France, is implemented due to the developed in axial direction annular seals.

There is a seal with a ring among the types of annular seals. Such seals are widely used as a sealing element to minimize liquid flow-over. Rings (they are often called floating ones) because of their initial self-centering, during operation allow providing parallel clearance between the case and the rotating shaft. The ring is usually fixed and resiliently pressed to the stator in order to prevent the axial displacements and create the initial sealing effect, while there is no pressure difference. When the shaft rotates, appearing in the seal slit hydrodynamic force tends to move the ring in radial direction. Friction force impedes the ring motion. If hydrodynamic force exceeds friction force, the ring starts moving after the rotor. As soon as hydrodynamic force becomes lower than sliding friction force, the

ring begin stopping. The ring may fix with eccentricity relative to the shaft.

There are a lot of works of Russian and foreign authors where the issues to provide the working capacity of such seals are considered. In work [3] calculation of minimum force of the spring prepressure that prevents the ring angular oscillations at all operating regimes is given. In work [4] calculation of possible contact between the rotor and the stator is presented. This may lead to depletion, rubbing and wear of the seal elements. Conditions for both appearance of running-in regime and reasons for these effects are given.

One of the most important tasks in modeling of the turbopumps rotors is obtaining of hydrodynamic force in an annular seal. Physical explanation for the origin of the radial hydrodynamic centering force in an annular seal was first given by A.A. Lomakin in 1953[5]. The earlier work where seals influence on the rotors dynamics was investigated is work of Rudis and Marcinkovskiy. [6]. Black was the first person abroad who explained influence of forces in an annular seal on dynamics of the turbine compressor rotor and obtained its dynamic coefficients [7, 8]. Childs and Andrés continued the mathematical models development, held investigations on annular seals work and checked them experimentally[9], [10]. These models are built for conditions of turbulent flow and allow obtaining both hydrodynamic forces and dynamic coefficients of stiffness and damping.

The aim of the present work is development of the methodology and the mathematical model of the seal with the floating ring and their application to the dynamics tasks of high-speed rotors. Analysis of the rotor system model is held in the DYNAMICS R4 program system (www.alfatran.com).

Geometry of annular seal

At the initial time moment the floating ring is considered fixed and centered, i.e. the seal works as an ordinary annular one. The ring starts moving when hydrodynamic force overcomes static friction force.

Figure 2 shows geometry of the equivalent ring where a floating ring of any other shape may be adjusted, and also forces acting on it at any time moment are given:

- P_1 – force from liquid pressure at the seal input;
- P_2 - force from liquid pressure at the seal output;
- F_ω - inertia force of the floating ring;
- F_g – hydrodynamic force in the seal slit;
- F_s – force from the spring action;
- F_r – reaction force appearing on the ring from pressure difference P_1 and P_2 and the spring;
- F_μ - friction force on contact surface of the ring and the case;

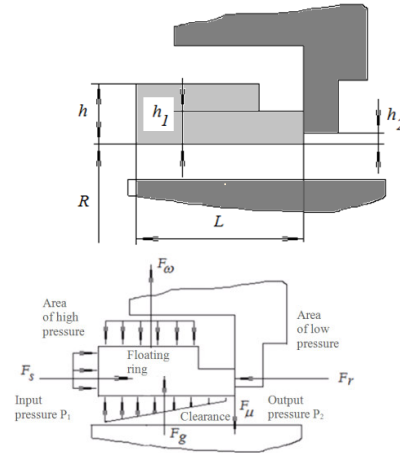


Figure 2. Geometry of equivalent ring and forces acting on it

Let us note some assumptions accepted for this ring model. The ring is considered to be ideal, without any diffuser or confuser shape. Inequality of clearance between the ring and the shaft, the form deviation of the seal faces at longitudinal and transverse direction are not taken into consideration. Change in friction force at change in contact area of the ring with the case is not considered if the ring moves.

Model of rotor system with ring

Figure 3 shows the scheme of the simplified rotor model with the floating ring. The rotor of 7.24 kg total mass is mounted and rotates in the rigid case on two supports - links 1, 2. Radial stiffness of the supports is $0.1 \cdot 10^9$ N/m, damping in the supports - 200 N·s/m. The rotor case is fixed on two supports – they are simulated by the absolutely rigid links 3 and 4. Unbalance of 0.5 g·cm is applied to the central shaft part.

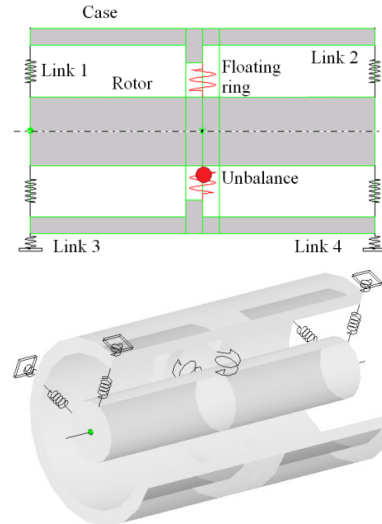


Figure 3. Model of rotor system with floating ring (two-dimensional and three-dimensional ones)

Table 1 gives the parameters of the annular part of the seal. Pressure P_1 and P_2 increase according to the

parabolic law, starting from the minimum pressure difference of 0.05 MPa up to one shown in Table.

Table 1

Slit		
Parameter	Value	Description
R	20	Shaft radius, mm
L	7.5	Slit length, mm
$\mu_{\text{ж}}$	13.8e-6	Dynamic viscosity (liquid hydrogen), Pa·s
ρ	70.8	Liquid density, kg/m ³
P_1	7.013e+6	Input pressure at 90000 rpm, MPa
P_2	0.755e+6	Output pressure at 90000 rpm, MPa
δ	0.027	Radial clearance, mm
α	0.5	Coefficient of liquid twist at seal input
ζ	0.1	Loss factor at seal input

Table 2 presents the ring parameters. Coefficients of static and sliding friction are accepted to be equal.

Table 2

Ring		
Parameter	Value	Description
m_{ring}	45	Ring mass, g
h_1	1.7	Ring thickness in contact area with case, mm
h_2	0.5	Ring thickness without contact with case, mm
μ_{rest}	0.1	Friction force factor
μ_{sliding}	0.1	Sliding friction factor
F_s	10	Prepressure force from spring, N
v_{min}	1	Minimum speed of ring sliding, mm/s

Linear analysis of rotor system

Use of the linear model allows obtaining natural frequencies and mode shapes of the rotor system at regimes and determining its stability boundary at change in logarithmic decrement of mode shapes.

The seal reaction on the dynamic system is defined by hydrodynamic force appearing in the seal slit. In linear analysis the ring is fixed, and the seal is an ordinary annular one.

Taking this into account, the rotor general motion equation in the matrix form and at linearized statement may be written as the following

$$[M]\{\ddot{q}\} + [C]\{\dot{q}\} + [K]\{q\} = \{F\}_{\delta\delta} + \{R^{seal}\}, \quad (1)$$

where

$[M]$, $[C]$, $[K]$ – square matrixes of inertia, damping and gyroscopic forces, and stiffness correspondingly, obtained for the finite-element model; $\{\ddot{q}\}$, $\{\dot{q}\}$, $\{q\}$ – column vectors of generalized accelerations, speeds and displacements correspondingly; $\{F_{\delta\delta}\}$ – column vector of unbalanced forces; $\{R^{seal}\}$ – column vector of the seal reaction.

To obtain hydrodynamic force, any algorithm connecting its value with the shaft displacements and speeds may be applied. Later, Childs algorithm will be used [9]. There hydrodynamic force is defined through stiffness and damping coefficients K_{xx} , K_{xy} and C_{xx} , C_{xy} . These coefficients are function of the seal geometry, the rotor speed, liquid characteristics, pressure difference and obtained for the central rotor position in clearance.

$$\begin{Bmatrix} R_x^{seal} \\ R_y^{seal} \end{Bmatrix} = - \begin{bmatrix} K_{xx} & K_{xy} \\ -K_{yx} & K_{yy} \end{bmatrix} \begin{Bmatrix} X \\ Y \end{Bmatrix} - \begin{bmatrix} C_{xx} & C_{xy} \\ -C_{yx} & C_{yy} \end{bmatrix} \begin{Bmatrix} \dot{X} \\ \dot{Y} \end{Bmatrix}.$$

Figure 4 shows change in stiffness and damping coefficients of the seal in the investigated range of the rotating speeds.

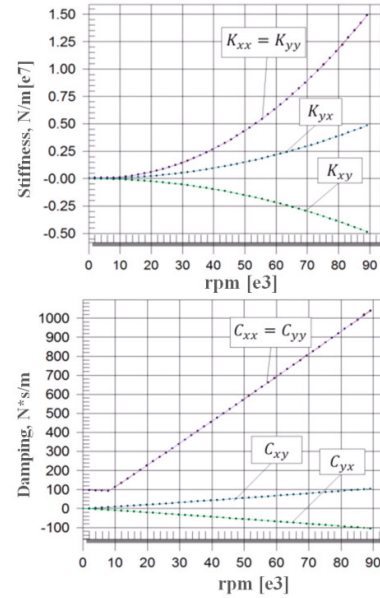


Figure 4. Characteristics of stiffness and damping coefficients

Apparently, cross-sectional stiffness and damping coefficients have the same value but different signs which indicates possible stability loss of the rotor and necessity to determine its boundary.

Figure 5 shows the obtained natural frequencies map (Campbell diagram) of the rotor system in the range up to 90000 rpm. In the investigated range of natural frequencies up to 225000 1/min for the non-rotating rotor, there are two natural frequencies. At rotation these frequencies are divided into frequencies corresponding to the forward precession (ascending diagram legs) and backward one (descending diagram legs). The first two frequencies merge into one line. The rotor mode shapes corresponding to these frequencies are shown on the map.

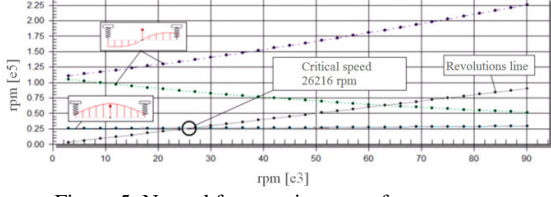


Figure 5. Natural frequencies map of rotor system

Figure 6 presents change in logarithmic decrement for the obtained mode shapes. Figure shows that the system loses stability when logarithmic decrement changes its value to negative one, i.e. at ~60750 rpm.

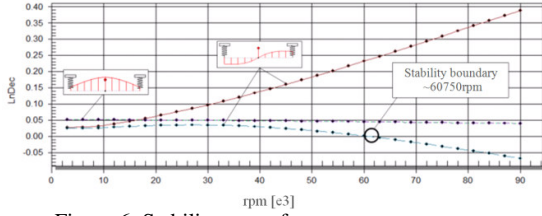


Figure 6. Stability map of rotor system

Natural frequency which the rotor loses stability at, may be obtained from the diagram of logarithmic decrement vs natural frequencies, Figure 7. Stability loss takes place at natural frequency of 27577 1/min and the mode shape shown in Figure.

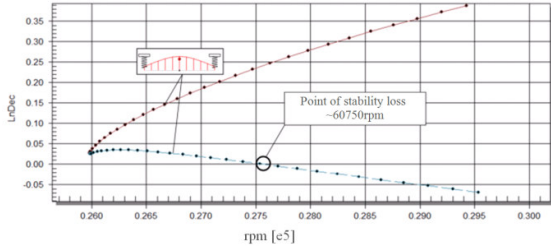


Figure 7 Diagram of logarithmic decrement vs natural frequencies map

Nonlinear analysis of rotor system

It is supposed that the ring has inertia and can move, i.e. the rotor system becomes nonlinear. So, the equation (1) is solved by its direct integrating with determination of the seal reaction at any integration step.

Let us consider the algorithm of determination of the seal reaction $\{R^{seal}\}$ on the rotor shaft motion. At initial time moment the seal ring is regarded as fixed and centered, i.e. the seal works as an ordinary annular one. The ring starts moving when hydrodynamic force overcomes static friction force.

$$|\bar{F}_g| > F_\mu^{rest}$$

Static and sliding friction force are calculated as

$$\begin{aligned} F_\mu^{rest} &= \mu_{rest} * F_r; \\ F_\mu^{sliding} &= \mu_{sliding} * F_r; \\ F_r &= (P_1 * S_{h1} - P_2 * S_{h2} + F_s), \end{aligned}$$

where μ_{rest} and $\mu_{sliding}$ – factors of static and sliding friction force correspondingly; S_{h1} and S_{h2} – areas corresponding to the ring sizes h_1 and h_2 .

If the ring speed is lower than minimum sliding speed, it is considered fixed:

$$|\bar{v}_n^{ring}| < v_{min}.$$

There are three modes which the ring may be found. The first one – when the ring is motionless. Vector of the ring reaction in the seal is equal but opposite in direction to the vector of hydrodynamic force in the slit:

$$\bar{R}^{seal} = -\bar{F}_g.$$

The second mode is when the ring is motionless but hydrodynamic force becomes equal to the static friction force. Then the ring reaction

$$\bar{R}^{seal} = -\bar{F}_\mu^{rest}.$$

and the ring gets acceleration

$$\bar{a}_n^{ring} = \bar{F}_\omega / m^{ring},$$

where m^{ring} – the ring mass; $\bar{F}_\omega = (\bar{F}_g - \bar{F}_\mu^{rest})$.

The third one is when the ring starts moving with acceleration. Reaction vector at its value is equal to static friction force

$$\bar{R}^{seal} = -\bar{F}_\mu^{sliding}.$$

and moves with acceleration

$$\bar{a}_n^{ring} = (\bar{F}_g - \bar{F}_\mu^{sliding}) / m^{ring}.$$

With consideration of the shaft and the ring displacements from the central position and their speed, the value of hydrodynamic force at X and Y projections may be defined through stiffness and damping coefficients K_{xx}, K_{xy} and C_{xx}, C_{xy} correspondingly, obtained for the central rotor position in clearance.

$$\begin{aligned} F_{gx} &= -(K_{xx} * \Delta u_x + K_{xy} * \Delta u_y + C_{xx} * \Delta v_x + C_{xy} * \Delta v_y); \\ F_{gy} &= -(K_{yx} * \Delta u_x + K_{yy} * \Delta u_y + C_{yx} * \Delta v_x + C_{yy} * \Delta v_y). \end{aligned}$$

where:

$$\begin{aligned} \Delta u_x &= u_x^{shaft} - u_x^{ring}; \Delta u_y = u_y^{shaft} - u_y^{ring}; \\ \Delta v_x &= v_x^{shaft} - v_x^{ring}; \Delta v_y = v_y^{shaft} - v_y^{ring}. \end{aligned}$$

The algorithm work on obtanment of the ring reaction may be presented as the block diagram, Figure 8. At initial time moment the ring has the central position. Input parameters for calculation of the ring reaction at n integration step are $u_x^{shaft}, u_y^{shaft}, v_x^{shaft}, v_y^{shaft}, \Delta t_n$.

Figure 9 shows the rotor amplitude-time characteristic at the place of the ring mounting. It is obtained during unsteady analysis using the above mentioned algorithm. Two areas of increased vibrations are highlighted – in the range of 26000-30000 rpm that corresponds to the first rotor critical speed and in the range from 83000 rpm that corresponds to the rotor stability loss from hydrodynamic forces in the seal.

Visual boundary of the rotor stability loss from hydrodynamic forces in the seal is about 83000 rpm. To adjust its position, the method described in [12] was used. At the constant regimes of 60000 rpm and 61000

rpm, impulse of 100 N was applied to the system for 0.01 s, Figure 10. Impulse of 60000 rpm does not lead to stability loss (amplitudes decay). Amplitudes from impulse action at 61000 rpm increase. It results from this that the boundary is in between these rotor speeds and close to the boundary obtained for the linear model.

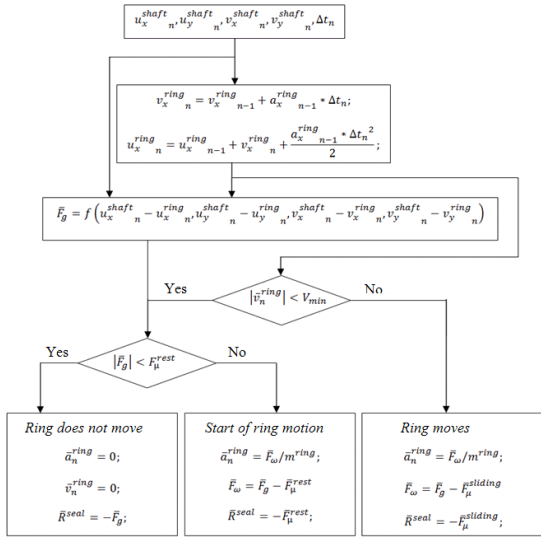


Figure 8. Block diagram of algorithm of seal reaction obtainment

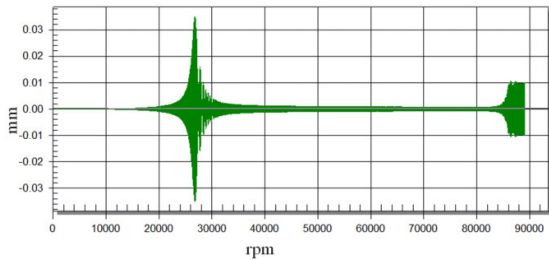


Figure 9. Amplitude-time rotor characteristic at displacement

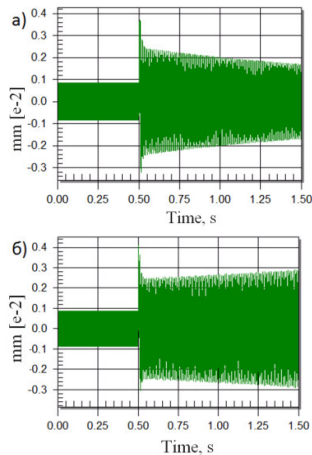


Figure 10. Time signal from impulse impact at 0.05s: a) up to stability boundary (60000 rpm), б) after (61000 rpm)

Maximum value of the rotor amplitude at resonance obtained at unsteady analysis (Figure 9) corresponds to the frequency ~ 26805 1/min, whereas at linear calculation critical speed is 26216 1/min, so the floating ring slightly toughened the rotor.

Conversion of the obtained time signal into the frequency one (Figure 11) shows that stability loss takes place at frequency 29297 1/min, that somewhat differs from the frequency obtained for linearized model - 27577 1/min.

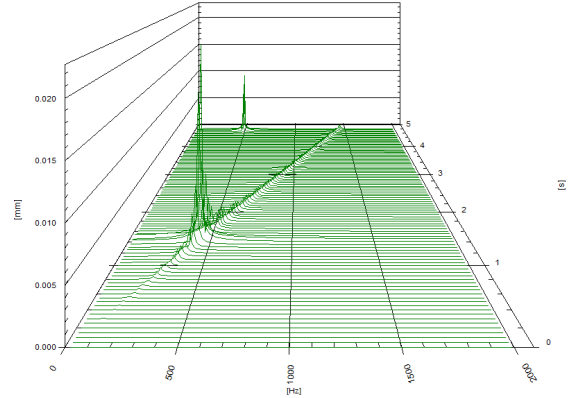


Figure 11. Cascade diagram of vibration spectra

Figure 12 shows change in the ring and friction force reaction at regimes. The ring reaction is limited by friction force.

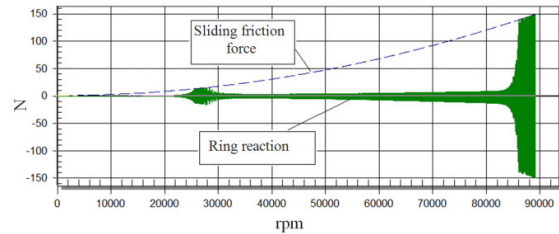


Figure 12 Reaction of ring and friction force

Figure 13 presents the ring motion at the resonance area.

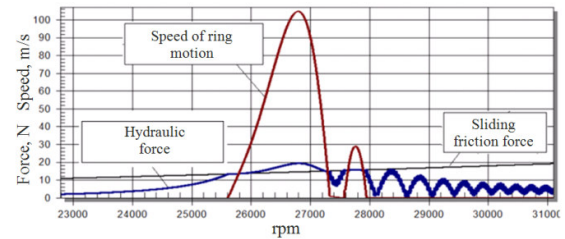


Figure 13. Ring motion when rotor passing resonance frequency

As the Figure shows, hydrodynamic force in clearance increases up to the value of static friction force. After that its value overcomes friction force, and the ring starts moving. The ring speed increases with increase in hydrodynamic force. When hydrodynamic force starts decreasing, the ring speed decreases. The ring stops with some eccentricity relatively the shaft

due to dominance of friction force over hydrodynamic one. In the sequel, the ring eccentricity causes some vibrations of hydrodynamic force. There may be several motion and stop cycles. In this case, there are only two ones.

Figure 14 shows in details the ring motion at area of stability loss from fluid flow, but this has just academic interest (the rotor operation close and after stability boundary is not allowed).

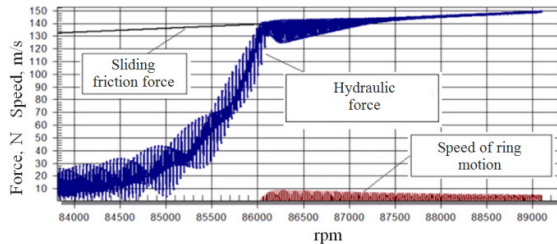


Figure 14. Ring motion in area of rotor's stability loss

Orbits of the ring motion at different regimes at time range 0.001 s are given below. The rotor motion at the stopped ring is circular one, Figure 15. Amplitudes of the rotor motion at stability loss increase up to the moment of the ring starting motion and then keep the level of 10 mkm, Figure 16 a. The ring amplitudes do not exceed 1.5 mkm, the motion pattern is interrupted, Figure 16 б. The areas of sharp bend of the ring motion trajectory are also noticeable.

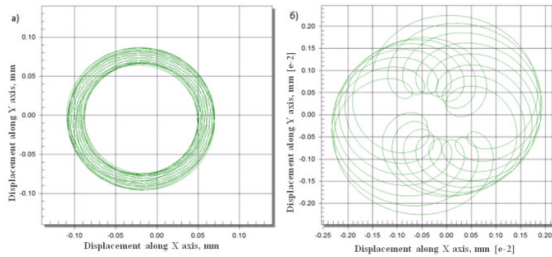


Figure 15. Rotor motion orbits (ring is fixed): a) at 83000 rpm; б) at 84500 rpm

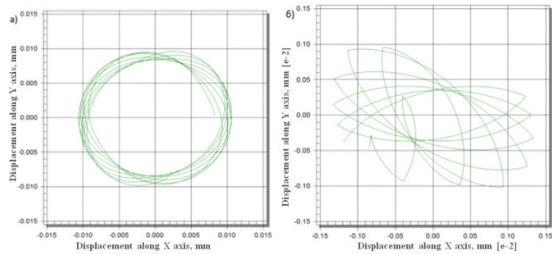


Figure 16. Motion orbits at 86000 rpm:

a) of rotor; б) of ring (motion start)

Figure 17 shows motion orbits at 89000 rpm. It should be noticed that the ring limits amplitudes of the rotor oscillations and does not allow their developing up to unsafe values.

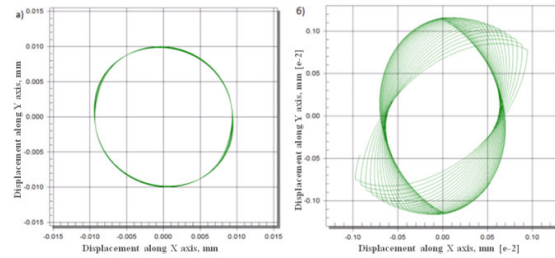


Figure 17. Motion orbits at 89000 rpm: a) of rotor; б) of ring

In the real seal construction under certain conditions, the contact between the rotor shaft and the ring may take place. This fact must be checked in any case. Figure 18 shows orbits of absolute shaft motion in the ring clearance at resonance within one cycle. The points are at initial position of the shaft and the ring and show the phase shift of vectors of the shaft and the ring displacements. In this case there is no contact.

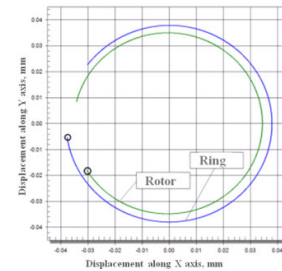


Figure 18. Check of contact between shaft with ring

Conclusions

The following main conclusions at the presented methodology and results of its application should be highlighted. The rotors analysis with annular seals may be hold both at stationary statement (linearized seal model) and unsteady one (nonlinear seal model).

At stationary statement the methodology allows considering unsymmetry of stiffness and damping matrixes of annular seals, obtaining amplitude-frequency rotor characteristics and defining the rotor stability boundary. At unsteady statement the methodology takes into account the ring inertia, hydrodynamic force in the slit, friction force of the ring about the case. It allows obtaining amplitude-time characteristics of the rotor shaft and the ring motion, defining trajectories of their motion, the ring behavior when passing resonance, checking possible contact between the shaft and the ring, defining the boundary of the rotor stability loss under hydrodynamic force.

The methodology also allows obtaining the necessary stiffness of the spring pressing the ring, adjusting the ring configuration, that the value of hydraulic force of the ring butt to the case depends on.

Literature

1. Иванов А.В. Турбонасосные агрегаты кислородно-водородных ЖРД: монография, Воронеж: ГОУВПО "Воронежский государственный технический университет", 2011. 283 с.
2. Герашенко Б.И. Динамика закритических роторов лопаточных машин. М.: Компания Спутник+, 2000 – 250 с.
3. Иванов А.В. Некоторые вопросы проектирования уплотнений с полуподвижными кольцами для насосов ТНА / А.В. Иванов // Разработка, производство и эксплуатация турбо-, электронасосных агрегатов и систем на их основе: труды I Международной научно-технической конференции "СИНТ'01". – Воронеж: ООО РИФ "Кварта", 2001. – С. 236 – 238.
4. Дмитренко А.И. Совершенствование уплотнений с полуподвижными кольцами для проточной части насосов ТНА ЖРД / А.И. Дмитренко, А.В. Иванов, А.Г. Кравченко // Научно-технический юбилейный сборник. КБ химавтоматики. – ИПФ "Воронеж", 2001. – С. 357 – 363.
5. Бедчер Ф.С., Ломакин А.А. Определение критического числа оборотов ротора насоса с учетом сил, возникающих в уплотнениях// Паро- и газотурбостроение. – 1957. - Вып.5. - С. 249-269.
6. М. А. Рудис, В. А. Марцинковский, Некоторые вопросы динамики роторов центробежных насосов / Котлотурбостроение: сборник трудов ЦКТИ. – 1964. – Вып. 44.
7. H. Black, Effects of Hydraulic Forces on Annular Pressure Seals on the Vibrations of Centrifugal Pump Rotors, Journal of Mechanical Engineering Science, 1969, 11(2), pp. 206-213.
8. Black, H. F., Jenssen, D. N., Dynamic Hybrid Bearing Characteristics of Annular Controlled Leakage Seals, Proc Instn Mech Engrs, 1970, Vol. 184, pp. 92-100.
9. Childs D.W. "Turbomachinery rotordynamics: phenomena, modeling and analysis". JOHN WILLEY & SONS, INC.1993. pp. 476.
10. L. San Andrés, Analysis of Variable Fluid Properties, Turbulent Annular Seals, ASME Journal of Tribology, 113, pp. 694-702, 1991.
11. Леонтьев М.К., Иванов А.В. Модальный анализ динамических систем роторов. "Известия высших учебных заведений. Авиационная техника". 2005, №3. С. 31-35.
12. Леонтьев М.К., Дегтярев С.А., Давыдов А.В., «Динамическая устойчивость ротора турбогенератора», журнал «Газотурбинные технологии», №4 2012 г.